

## Synthesis and crystal structure of $\text{MgB}_{12}$

Volker Adasch<sup>a</sup>, Kai-Uwe Hess<sup>b</sup>, Thilo Ludwig<sup>c,d</sup>, Natascha Vojteer<sup>c,d</sup>, Harald Hillebrecht<sup>c,d,\*</sup>

<sup>a</sup>DRONCO AG, Wiesenmühle 1, D-95632 Wunsiedel, Germany

<sup>b</sup>Ludwig-Maximilians-Universität München, Institut für Mineralogie, Petrologie und Geochemie, Theresienstr. 41/III, D-80333 München, Germany

<sup>c</sup>Albert-Ludwigs-Universität Freiburg, Institut für Anorganische und Analytische Chemie, Albertstr. 21, D-79104 Freiburg, Germany

<sup>d</sup>Freiburger Materialforschungszentrum FMF, Stefan-Maier-Str. 25, D-79104 Freiburg, Germany

Received 18 September 2005; received in revised form 15 March 2006; accepted 22 March 2006

Available online 22 May 2006

### Abstract

Single crystals of  $\text{MgB}_{12}$  were synthesized from the elements in a Mg/Cu melt at 1600 °C.  $\text{MgB}_{12}$  crystallizes orthorhombic in space group  $Pnma$  with  $a = 16.632(3)$  Å,  $b = 17.803(4)$  Å and  $c = 10.396(2)$  Å. The crystal structure ( $Z = 30$ , 5796 reflections, 510 variables,  $R_1(F) = 0.049$ ,  $wR_2(I) = 0.134$ ) consists of a three dimensional net of  $\text{B}_{12}$  icosahedra and  $\text{B}_{21}$  units in a ratio 2:1. The  $\text{B}_{21}$  units are observed for the first time in a solid compound. Mg is on positions with partial occupation. The summation reveals the composition  $\text{MgB}_{12.35}$  or  $\text{Mg}_{0.97}\text{B}_{12}$ , respectively. This is in good agreement with the value of  $\text{MgB}_{11.25}$  as expected by electronic reasons to stabilize the boron polyhedra  $\text{B}_{12}^{2-}$  and  $\text{B}_{21}^{4-}$ .

© 2006 Elsevier Inc. All rights reserved.

**Keywords:** Synthesis; Single crystals; Structure analysis; Magnesium boride; Boron rich boride;  $\text{B}_{21}$  unit; WDX measurements

### 1. Introduction

Since the surprising observation of superconductivity in  $\text{MgB}_2$  [1] with  $T_c = 39$  K the interest in magnesium borides has grown dramatically. But already some time before, on the basis of theoretical calculations metal doped  $\beta$ -rhombohedral boron like  $\text{LiB}_{\sim 13}$  [2a] and  $\text{MgB}_{\sim 20}$  [2b] were proposed to be high  $T_c$  superconductors. The published phase diagram Mg/B [3] shows beside  $\text{MgB}_2$  and  $\text{MgB}_4$  the boron rich compounds  $\text{MgB}_7$  and  $\text{MgB}_{20}$ . There are some hints for the existence of a compound  $\text{MgB}_{12}$  [4] but its existence is denied by recent investigations of Brutti et al. [5].

In this work we report on synthesis and crystal structure of a new Mg boride  $\text{MgB}_{12}$ . In a proceeding contribution [6] we report on the synthesis of single crystals of boron rich borides of magnesium using Mg/Cu melts.

### 2. Experimental

Single crystals of  $\text{MgB}_{12}$  were synthesized from the elements in a Cu/Mg melt. Cu, Mg and B were mixed in molar ratios 5:3:2 and pressed into a pellet (ca. 2 g). The pellet was put into a BN-crucible and the crucible in a Ta-ampoule, which was sealed by welding with an electric arc. The ampoule was heated in an argon atmosphere up to 1600 °C held for 40 h, cooled with 10 K/h to 800 °C and with 100 K/h to room temperature. The ampoule was opened and the excess melt dissolved in concentrated nitric acid. Single crystals of  $\text{MgB}_{12}$  were of bluish-black colour and irregular shape. As by-product dark red to black single crystals of  $\text{MgB}_7$  [6,7] and in some cases  $\text{MgB}_{20}$  [6] were observed. Furthermore  $\text{MgB}_{12}$  was observed as a by-product in the course of investigations on boridecarbides of magnesium [8].

Qualitative and quantitative analyses on selected single crystals were done by EDX and WDX measurements. Several single crystals were checked by EDX (Jeol, JSM 6400 with Ge detector, sample fixed with conducting glue on a graphite platelet mounted on a Al sample holder). It confirmed magnesium as the only heavy element ( $Z > 10$ ).

\*Corresponding author. Fax: +49 761 203 6102.

E-mail address: [harald.hillebrecht@ac.uni-freiburg.de](mailto:harald.hillebrecht@ac.uni-freiburg.de) (H. Hillebrecht).

By WDX (Jeol, JXA 8200) a more detailed analysis with special consideration of light elements ( $4 < Z < 11$ ) was done to exclude its incorporation (especially carbon), which occurs frequently in boron rich borides.

For the WDX measurements single crystals were fixed in a matrix with Cu/epoxy resin and polished to get a clear surface and to secure the measurement on the interior of the crystal [8] and not the surface which may be influenced by the contact to the melt. Boron and magnesium were detected as the only elements with  $Z > 4$ . The molar ratio B:Mg was found to be 91.9:8.1 leading to the composition  $\text{MgB}_{12.4}$  in excellent agreement with the composition determined by X-ray methods.

### 2.1. Structure solution and refinement

Investigations with a single crystal diffractometer equipped with  $\text{MoK}\alpha$  radiation and an image plate detector (Fa. Stoe, IPDS II) revealed a primitive orthorhombic unit cell with  $a = 16.632(3) \text{ \AA}$ ,  $b = 17.803(4) \text{ \AA}$  and  $c = 10.396(2) \text{ \AA}$ . Measurement of 35,288 intensities gave a data set of 5796 independent reflections (4752 with  $I > 2\sigma(I)$ ). The special reflection conditions were  $k + l = 2n$  for reflections  $h0l$  and  $h = 2n$  for reflections  $hk0$  leading to the possible space groups  $Pnma$  and  $Pna2_1$ . The structure solution was started in  $Pnma$ . Direct methods (SHELXTL [9]) revealed the position of most of B- and Mg atoms. Missing atoms were localized by subsequent difference Fourier syntheses. The labelling B/Mg was done according to bonding distances and electron densities. It turned out that all boron positions were fully occupied while the Mg positions show partial occupation factors with values between 82.9(5)% and 13.6(3)%. Mg5/Mg9 are refined with split positions. The symmetry reduction to  $Pna2_1$  did not improve the quality of refinement significantly. Occupation factors for boron were between 96.4(19)% and 104.8(15)%, therefore full occupations were assumed. In total there are 51 positions for boron and 9 for magnesium. The unit cell contains 30 formula units. The sum of the occupation factors leads to the composition  $\text{MgB}_{12.35}$ . Regarding the fact that the partial occupation refers to the Mg atoms the composition  $\text{Mg}_{29.14}\text{B}_{360}$  or  $\text{Mg}_{0.97}\text{B}_{12}$ , respectively, seems to be more adequate. To simplify matters we still keep the formulation  $\text{MgB}_{12}$  for the following discussions.

Because of the low absorption coefficient ( $0.23 \text{ mm}^{-1}$ ) no correction of absorption effects was done. Finally  $R$ -values of  $R_1(F) = 0.049$  and  $wR_2(I) = 0.134$  were yielded for 5796 reflections and 510 free variables. All atoms were refined with anisotropic thermal displacement parameters. Despite the low electron number of boron the values  $U_{\text{equ}}$  and  $U_{ij}$  of the 51 boron atoms are small and nearly equal confirming correct assignment, full occupation and a well ordered boron partial structure. The values for the Mg atoms show more differences according to the disorder and the small values for the occupation factors. These findings were confirmed for several crystals (lattice constants,

Table 1  
Details of the crystal structure determination

Crystal shape and colour	Irregular polyhedron, bluish-black
Crystal dimensions	$0.3 \times 0.4 \times 0.5 \text{ mm}^3$
Crystal system	Orthorhombic
Space group	$Pnma$
Lattice constants	$a = 16.632(3) \text{ \AA}$ , $b = 17.802(4) \text{ \AA}$ , $c = 10.396(2) \text{ \AA}$
Cell volume	$3077.94 \text{ \AA}^3$
No. of formula units	30
Composition in unit cell	$\text{Mg}_{29.15}\text{B}_{360}$
Density calculated	$2.480 \text{ g/cm}^3$
Radiation	$\text{Mo-K}\alpha$ (IPDS II), graphite monochromator
Range ( $hkl$ )	$-25 \leq h \leq 24$ , $-24 \leq k \leq 27$ , $-15 \leq l \leq 15$
Range ( $2\theta$ )	$7\text{--}65.64^\circ$
Temperature of measurement	$21^\circ \text{C}$
Scan modus/measurement	90 frames and 8 min with $2^\circ\phi$ increment
Reflections measured	35,288
Unique reflections	5796 (4752 with $I > 2\sigma$ )
Internal $R$ -value	0.0844 ( $\sigma = 0.0451$ )
Absorption coefficient	$0.23 \text{ mm}^{-1}$
Absorption correction	None
Structure solution	Direct methods/SHELXTL [9]
Refinement	SHELXTL [9]
Residual electron density	$+0.84 \text{ e}^-/\text{\AA}^3$ , $-0.40 \text{ e}^-/\text{\AA}^3$ ( $\sigma = 0.10 \text{ e}^-/\text{\AA}^3$ )
Weighting function	$1/[\sigma^2(F_o^2) + (0.0642P)^2 + 0.00P]$ with $P = (F_o^2 + 2F_c^2)/3$
Number of parameters	510
$R$ values	$R_1(F) = 0.049$ , $wR_2(I) = 0.134$

symmetry, fully occupied boron sites, partial occupation of magnesium sites, composition). The differences were covered by the standard deviations given in the tables. Details for the best refinement of a single crystal are listed in Table 1. Coordinates and thermal displacement parameters are given in Table 2. Selected distances are shown in Tables 3–7. Further details on the structure refinement (anisotropic thermal displacement parameters, complete list of distances and angles,  $F_o/F_c$ -list) may be obtained from: Fachinformationszentrum Karlsruhe, D-76344 Eggenstein-Leopoldshafen (Germany) (fax: +49 724 808 666; e-mail: [crysdata@fiz-karlsruhe.de](mailto:crysdata@fiz-karlsruhe.de)) on quoting the registry number CSD-416351.

## 3. Results and discussion

### 3.1. Crystal structure of $\text{MgB}_{12}$

The crystal structure of  $\text{MgB}_{12}$  shows the typical structural features of boron rich borides. The boron atoms form a three-dimensional (3D) network of polyhedra and the metal atoms are located on positions in between with partial occupation. There are two different types of polyhedra in a ratio of 2:1, namely  $\text{B}_{12}$  icosahedra and  $\text{B}_{21}$  polyhedra (Fig. 1). The  $\text{B}_{21}$  polyhedra consist of two icosahedra sharing a common face. One apex is missing and the vertex B51–B513 is capped by an additional boron

Table 2  
Coordinates, thermal displacement parameters (in  $\text{\AA}^2$ ) and site occupation factors

Atom	Site	x	y	z	$U_{\text{eq}}$	Occupation factor
Mg1	4c	0.12656(6)	0.75	0.33373(10)	0.0158(3)	0.829(5)
Mg2	8d	0.48110(5)	0.55916(4)	0.16658(7)	0.0123(2)	0.738(4)
Mg3	8d	0.33702(4)	0.63076(4)	0.45857(7)	0.0140(3)	0.765(4)
Mg4	4c	0.2608(2)	0.75	0.4517(2)	0.0249(9)	0.186(3)
Mg5	8d	0.3047(2)	0.4335(1)	0.6206(1)	0.0235(6)	0.656(9)
Mg6	8d	0.3325(2)	0.5782(2)	0.6344(4)	0.0095(12)	0.136(3)
Mg7	8d	0.3491(1)	0.5614(1)	0.2641(2)	0.0105(8)	0.225(3)
Mg8	8d	0.5794(1)	0.6292(1)	0.2649(2)	0.0107(8)	0.217(3)
Mg9	8d	0.2612(6)	0.4408(2)	0.6447(3)	0.0355(18)	0.307(9)
B11	4c	0.1653(1)	0.25	0.6266(2)	0.0104(4)	1
B12	8d	0.3330(1)	0.6983(1)	0.2681(2)	0.0113(3)	1
B13	8d	0.3897(1)	0.6659(1)	1.1268(2)	0.0114(3)	1
B14	4c	0.0794(1)	0.25	0.5379(2)	0.0104(4)	1
B15	4c	0.4027(1)	0.75	0.3750(2)	0.0113(4)	1
B16	8d	0.4921(1)	0.6985(1)	1.1344(2)	0.0113(3)	1
B17	8d	0.9391(1)	0.6645(1)	0.2117(2)	0.0116(3)	1
B18	4c	0.0011(1)	0.75	0.2076(2)	0.0117(4)	1
B21	4c	0.3127(1)	0.75	0.7935(2)	0.0114(4)	1
B22	8d	0.3169(1)	0.6990(1)	0.6470(2)	0.0117(3)	1
B23	8d	0.3739(1)	0.6692(1)	0.7862(2)	0.0110(3)	1
B24	4c	0.0924(1)	0.25	0.3749(2)	0.0110(4)	1
B25	4c	0.3929(1)	0.75	0.5440(2)	0.0115(4)	1
B26	8d	0.4241(1)	0.6666(1)	0.6344(2)	0.0114(3)	1
B27	8d	0.0254(1)	0.3002(1)	0.2775(2)	0.0107(3)	1
B28	4c	0.5169(1)	0.25	0.3690(2)	0.0111(4)	1
B31	8d	0.5301(1)	0.4282(1)	0.6089(2)	0.0114(3)	1
B32	8d	0.4424(1)	0.4179(1)	0.5106(2)	0.0113(3)	1
B33	8d	0.4388(1)	0.4915(1)	0.6404(2)	0.0119(3)	1
B34	8d	0.5410(1)	0.5322(1)	0.6448(2)	0.0115(3)	1
B35	8d	0.3953(1)	0.5097(1)	0.4758(2)	0.0116(3)	1
B36	8d	0.4584(1)	0.5826(1)	0.5650(2)	0.0115(3)	1
B41	8d	0.3196(1)	0.3018(1)	0.6427(2)	0.0115(3)	1
B42	4c	0.0853(1)	0.75	0.1128(2)	0.0114(4)	1
B43	8d	0.3913(1)	0.3337(1)	0.5161(2)	0.0112(3)	1
B44	8d	0.2866(1)	0.3325(1)	0.4837(2)	0.0114(3)	1
B45	4c	0.2505(1)	0.25	0.5552(2)	0.0110(4)	1
B46	4c	0.4291(1)	0.25	0.4450(2)	0.0110(4)	1
B47	8d	0.1478(1)	0.6994(1)	0.8634(2)	0.0109(3)	1
B48	4c	0.2357(1)	0.75	0.8931(2)	0.0106(4)	1
B51	8d	0.6763(1)	0.6480(1)	0.0530(2)	0.0116(3)	1
B52	8d	0.2119(1)	0.5619(1)	0.5268(2)	0.0113(3)	1
B53	8d	0.2236(1)	0.6519(1)	0.6058(2)	0.0111(3)	1
B54	8d	0.6310(1)	0.7026(1)	0.9250(2)	0.0108(3)	1
B55	8d	0.3861(1)	0.4384(1)	0.9397(2)	0.0113(3)	1
B56	8d	0.4357(1)	0.3501(1)	0.9675(2)	0.0111(3)	1
B57	8d	0.3730(1)	0.4892(1)	1.0859(2)	0.0118(3)	1
B58	8d	0.5315(1)	0.5687(1)	0.9323(2)	0.0113(3)	1
B59	8d	0.1970(1)	0.5667(1)	0.6938(2)	0.0118(5)	1
B510	8d	0.1435(1)	0.6523(1)	0.7241(2)	0.0110(3)	1
B511	8d	0.9515(1)	0.3460(1)	0.3538(2)	0.0115(3)	1
B512	8d	0.5858(1)	0.5664(1)	0.7838(2)	0.0110(3)	1
B513	8d	0.2832(1)	0.4377(1)	0.8498(2)	0.0120(3)	1
B514	8d	0.2642(1)	0.5354(1)	0.8108(2)	0.0111(3)	1
B515	8d	0.3768(1)	0.4975(1)	0.7975(2)	0.0115(3)	1
B516	8d	0.2839(1)	0.5064(1)	0.4482(2)	0.0115(3)	1
B517	8d	0.3510(1)	0.5902(1)	0.8637(2)	0.0113(3)	1
B518	8d	0.2346(1)	0.4137(1)	0.4562(2)	0.0119(3)	1
B519	8d	0.3615(1)	0.5860(1)	1.0386(2)	0.0113(3)	1
B520	8d	0.4302(1)	0.5411(1)	0.9355(2)	0.0126(3)	1
B521	8d	0.2295(1)	0.6564(1)	0.2939(2)	0.0115(3)	1

Table 3  
Endohedral distances (in [Å]) in B<sub>12</sub> icosahedra

B11–B12 <sup>a</sup> 1.736(3)	B12–B17 <sup>a</sup> 1.876(2)	B15–B18 1.848(3)
B11–B13 <sup>a</sup> 1.755(2)	B13–B14 <sup>a</sup> 1.833(2)	B16–B16 1.834(3)
B11–B14 1.700(3)	B13–B16 <sup>a</sup> 1.802(2)	B16–B17 <sup>a</sup> 1.924(2)
B12–B12 1.841(3)	B13–B17 <sup>a</sup> 1.870(2)	B16–B18 <sup>a</sup> 1.887(3)
B12–B13 <sup>a</sup> 1.839(2)	B14–B16 <sup>a</sup> 1.808(3)	B17–B18 <sup>a</sup> 1.838(2)
B12–B15 <sup>a</sup> 1.850(3)	B15–B17 <sup>a</sup> 1.869(2)	∅ B–B 1.833
B21–B22 <sup>a</sup> 1.774(3)	B22–B26 <sup>a</sup> 1.877(2)	B25–B28 1.752(3)
B21–B23 <sup>a</sup> 1.763(2)	B23–B24 <sup>a</sup> 1.798(2)	B26–B27 <sup>a</sup> 1.808(2)
B21–B24 1.791(3)	B23–B26 <sup>a</sup> 1.786(2)	B26–B28 <sup>a</sup> 1.779(2)
B22–B22 1.816(3)	B23–B27 <sup>a</sup> 1.765(2)	B27–B27 1.786(3)
B22–B23 <sup>a</sup> 1.810(2)	B24–B27 <sup>a</sup> 1.750(3)	B27–B28 <sup>a</sup> 1.771(3)
B22–B25 <sup>a</sup> 1.887(3)	B25–B26 <sup>a</sup> 1.832(2)	∅ B–B 1.798
B31–B32 <sup>a</sup> 1.790(2)	B32–B33 <sup>a</sup> 1.881(2)	B33–B35 <sup>a</sup> 1.886(2)
B31–B33 <sup>a</sup> 1.918(2)	B32–B34 <sup>a</sup> 1.864(2)	B33–B36 <sup>a</sup> 1.831(2)
B31–B34 <sup>a</sup> 1.897(2)	B32–B35 <sup>a</sup> 1.846(2)	B34–B35 <sup>a</sup> 1.802(2)
B31–B35 <sup>a</sup> 1.881(2)	B32–B36 <sup>a</sup> 1.826(2)	B34–B36 <sup>a</sup> 1.838(2)
B31–B36 <sup>a</sup> 1.828(2)	B33–B34 <sup>a</sup> 1.847(2)	B35–B36 <sup>a</sup> 1.910(2)
∅ B–B 1.857		
B41–B41 1.845(3)	B42–B46 1.761(2)	B44–B48 <sup>a</sup> 1.782(3)
B41–B42 <sup>a</sup> 1.857(2)	B43–B44 <sup>a</sup> 1.773(2)	B45–B48 1.701(3)
B41–B43 <sup>a</sup> 1.863(2)	B43–B46 <sup>a</sup> 1.778(2)	B46–B47 <sup>a</sup> 1.779(2)
B41–B44 <sup>a</sup> 1.826(2)	B43–B47 <sup>a</sup> 1.813(2)	B47–B47 1.803(3)
B41–B45 <sup>a</sup> 1.733(3)	B44–B45 <sup>a</sup> 1.751(2)	B47–B48 <sup>a</sup> 1.745(3)
B42–B43 <sup>a</sup> 1.839(2)	B44–B47 <sup>a</sup> 1.754(2)	∅ B–B 1.790

<sup>a</sup>Distances occur two times.

Table 4  
Endohedral distances (in [Å]) in B<sub>21</sub>-unit

B51–B52 1.839(2)	B55–B57 1.782(2)	B513–B514 1.814(2)
B51–B53 1.830(2)	B55–B58 1.915(2)	B513–B515 1.964(2)
B51–B54 1.813(2)	B55–B513 1.950(2)	B513–B516 1.812(2)
B51–B55 1.854(2)	B55–B515 1.822(2)	B514–B515 1.996(2)
B51–B56 1.875(2)	B55–B520 1.973(2)	B514–B516 1.797(2)
B51–B513 1.948(2)	B56–B58 1.862(2)	B514–B517 1.828(2)
B52–B53 1.810(2)	B56–B511 1.877(2)	B514–B518 1.763(2)
B52–B55 1.864(2)	B57–B58 1.903(2)	B515–B517 1.838(2)
B52–B57 1.791(2)	B57–B59 1.900(2)	B515–B520 1.857(2)
B52–B59 1.757(2)	B57–B512 1.813(2)	B516–B518 1.843(2)
B52–B513 1.840(2)	B57–B519 1.800(2)	B517–B518 1.720(2)
B52–B516 1.754(2)	B57–B520 2.050(2)	B517–B519 1.829(2)
B53–B54 1.815(2)	B58–B511 1.745(2)	B517–B520 1.748(2)
B53–B59 1.825(2)	B58–B512 1.755(2)	B518–B519 1.815(2)
B53–B510 1.814(2)	B59–B510 1.791(2)	B519–B520 1.758(2)
B54–B56 1.833(2)	B59–B512 1.863(2)	B521–B51 1.827(2)
B54–B510 1.804(2)	B510–B511 1.777(2)	B521–B513 1.785(2)
B54–B511 1.784(2)	B510–B512 1.808(2)	∅ B–B 1.826
B55–B56 1.796(2)	B511–B512 1.829(2)	

atom (B521). This B<sub>21</sub> unit is observed for the first time in a boron rich boride. The crystal structure contains four different icosahedra (icosahedron 1: B11–B18, icosahedron 2: B21–B28, icosahedron 3: B31–B36, icosahedron 4: B41–B48) built by 30 independent boron atoms. The B<sub>21</sub> polyhedron is formed by 21 independent boron atoms (B51–B521).

The description of the complex crystal structure of MgB<sub>12</sub> can best be done by using the icosahedra as motifs. As shown in Fig. 2a the icosahedra form rods consisting of

Table 5  
Exohedral distances (in [Å]) of B<sub>12</sub> icosahedra

B11–B45 1.599(3)	B14–B24 1.708(3)	B17–B31 <sup>a</sup> 2.032(2)
B12–B521 <sup>a</sup> 1.895(2)	B15–B25 1.766(3)	B18–B42 1.712(3)
B13–B519 <sup>a</sup> 1.756(2)	B16–B56 <sup>a</sup> 1.820(2)	∅ B–B 1.816
B21–B48 1.649(3)	B24–B14 1.708(3)	B27–B511 <sup>a</sup> 1.676(2)
B22–B53 <sup>a</sup> 1.816(3)	B25–B15 1.766(3)	B28–B46 1.662(3)
B23–B517 <sup>a</sup> 1.665(2)	B26–B36 <sup>a</sup> 1.757(2)	∅ B–B 1.718
B31–B17 <sup>a</sup> 2.032(2)	B33–B515 <sup>a</sup> 1.934(2)	B35–B516 <sup>a</sup> 1.877(2)
B32–B43 <sup>a</sup> 1.727(2)	B34–B512 <sup>a</sup> 1.736(2)	B36–B26 <sup>a</sup> 1.757(2)
∅ B–B 1.844		
B41–B521 <sup>a</sup> 1.921(2)	B44–B518 <sup>a</sup> 1.709(2)	B47–B510 <sup>a</sup> 1.674(2)
B42–B18 1.712(3)	B45–B11 1.599(3)	B48–B21 1.649(3)
B43–B32 <sup>a</sup> 1.727(2)	B46–B28 1.662(3)	∅ B–B 1.724

<sup>a</sup>Distances occur two times.

Table 6  
Exohedral distances (in [Å]) of the B<sub>21</sub> unit

B51–B521 1.827(2)	B510–B47 1.674(2)	B516–B35 1.877(2)
B53–B22 1.816(3)	B511–B27 1.676(2)	B517–B23 1.665(2)
B54–B54 1.686(3)	B512–B34 1.734(2)	B518–B44 1.709(2)
B56–B16 1.820(2)	B513–B521 1.785(2)	B519–B13 1.756(2)
B58–B520 1.755(2)	B514–B59 1.744(2)	B520–B58 1.755(2)
B59–B514 1.744(2)	B515–B33 1.934(2)	∅ B–B 1.768

Table 7  
Mg–B distances (in [Å])

Mg1–B 2.318(2)–2.647(4) ∅:	Mg6–B 2.170(4)–2.459(4) ∅:	2.299 12x
2.444 14x		
Mg2–B 2.342(2)–2.597(2) ∅:	Mg7–B 2.290(3)–2.647(3) ∅:	2.468 14x
2.564 16x		
Mg3–B 2.317(2)–2.693(1) ∅:	Mg8–B 2.291(3)–2.839(3) ∅:	2.500 15x
2.474 15x		
Mg4–B 2.298(3)–2.710(3) ∅:	Mg9–B 2.065(3)–2.781(3) ∅:	2.502 13x
2.442 14x		
Mg5–B 2.184(2)–2.741(2) ∅:		
2.429 13x		

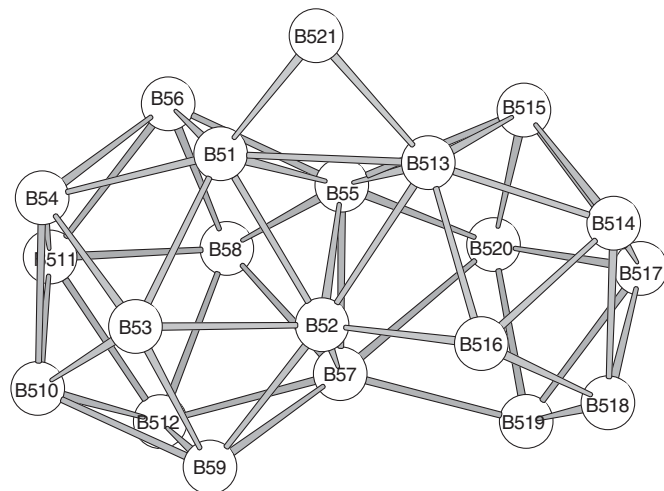


Fig. 1. B<sub>21</sub> unit in MgB<sub>12</sub>.

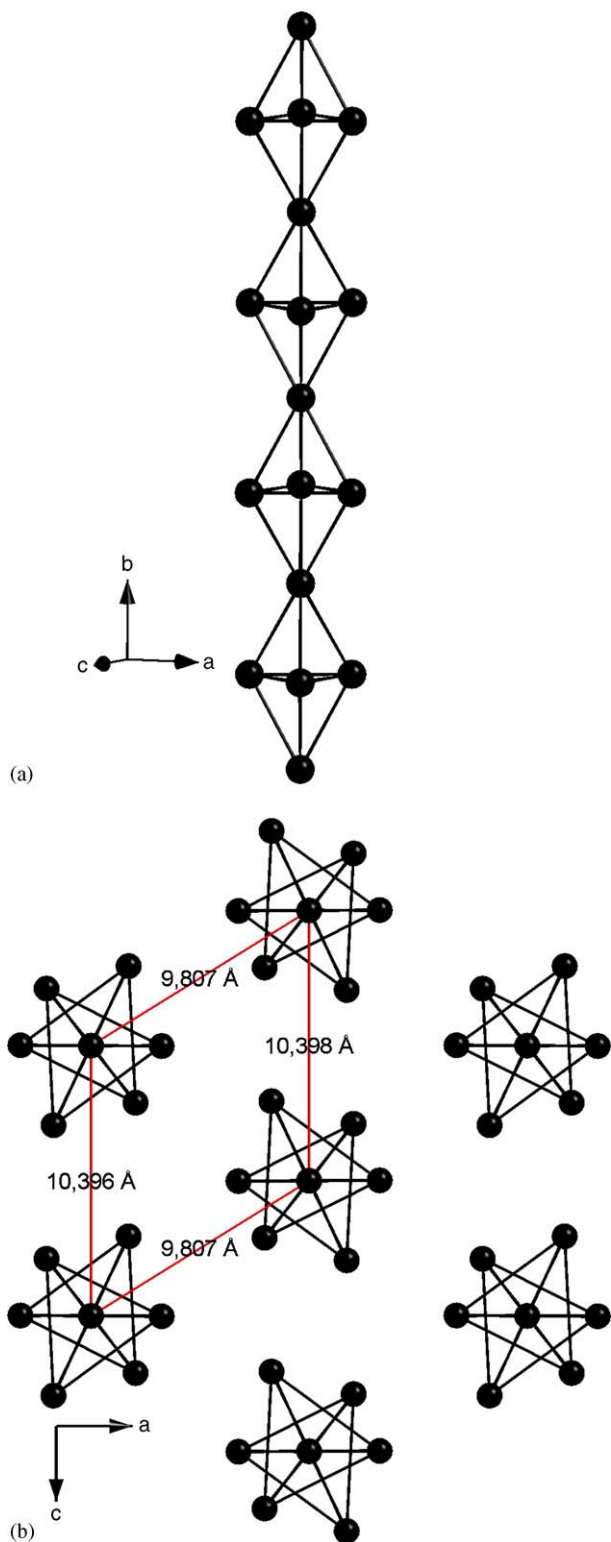


Fig. 2. (a) Chain of  $B_{12}$  icosahedra and (b) hexagonal rod packing; black circles represent  $B_{12}$  icosahedra.

alternating triangles of icosahedra (icosahedra 1, 2 and 4) and isolated icosahedra (icosahedron 3). The orientation of the triangles is nearly staggered relative to each other. The rods of icosahedra form a hexagonal rod packing with

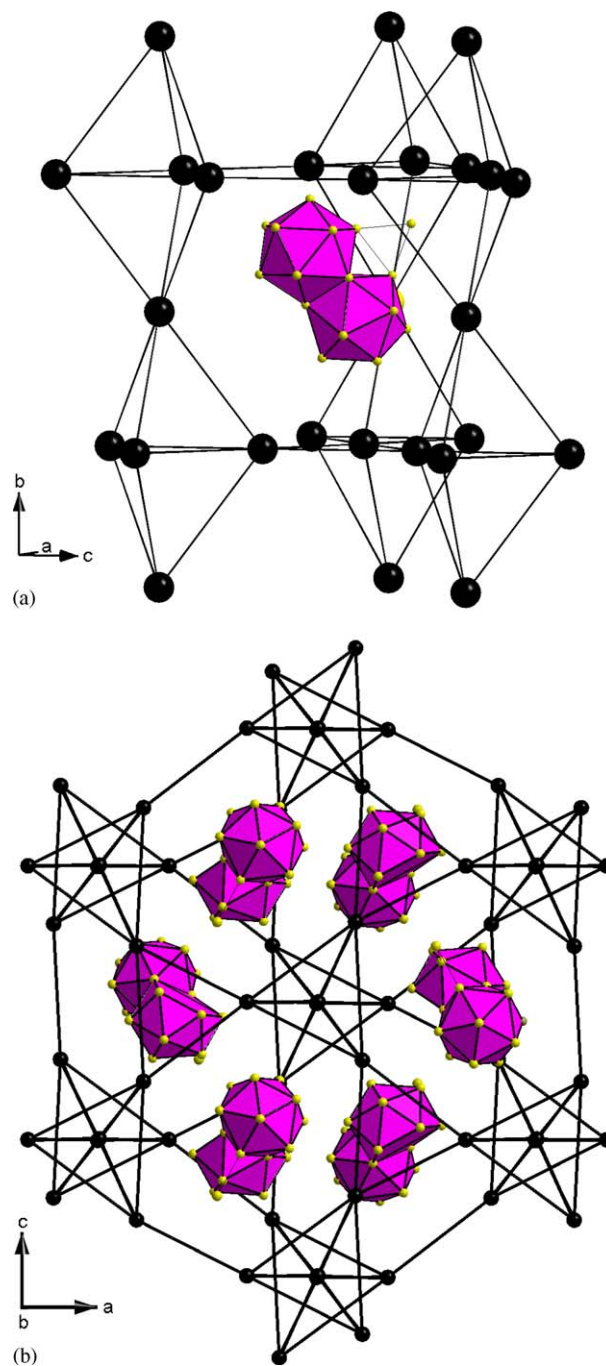


Fig. 3. (a)  $B_{21}$  unit in a void of the  $B_{12}$  icosahedra and (b)  $B_{21}$  units in the rod packing; black circles represent  $B_{12}$  icosahedra.

distances between the rods of about  $10 \text{ \AA}$  (Fig. 2b). This explains easily the pseudohexagonal metric of the  $a$ - $c$  plane ( $c/a = 1.60 \approx \sqrt{3}$ ). The rods are connected by exohedral bonds between the icosahedra of the triangles. The  $B_{21}$  units are placed in the holes between the icosahedra (Fig. 3a), which are trigonal prismatic voids with respect to the triangle centres. According to the stoichiometry all trigonal prismatic voids are occupied (Fig. 3b). In total every icosahedron has 6 exohedral bonds to another icosahedron and 6 exohedral bonds to a  $B_{21}$  unit. The

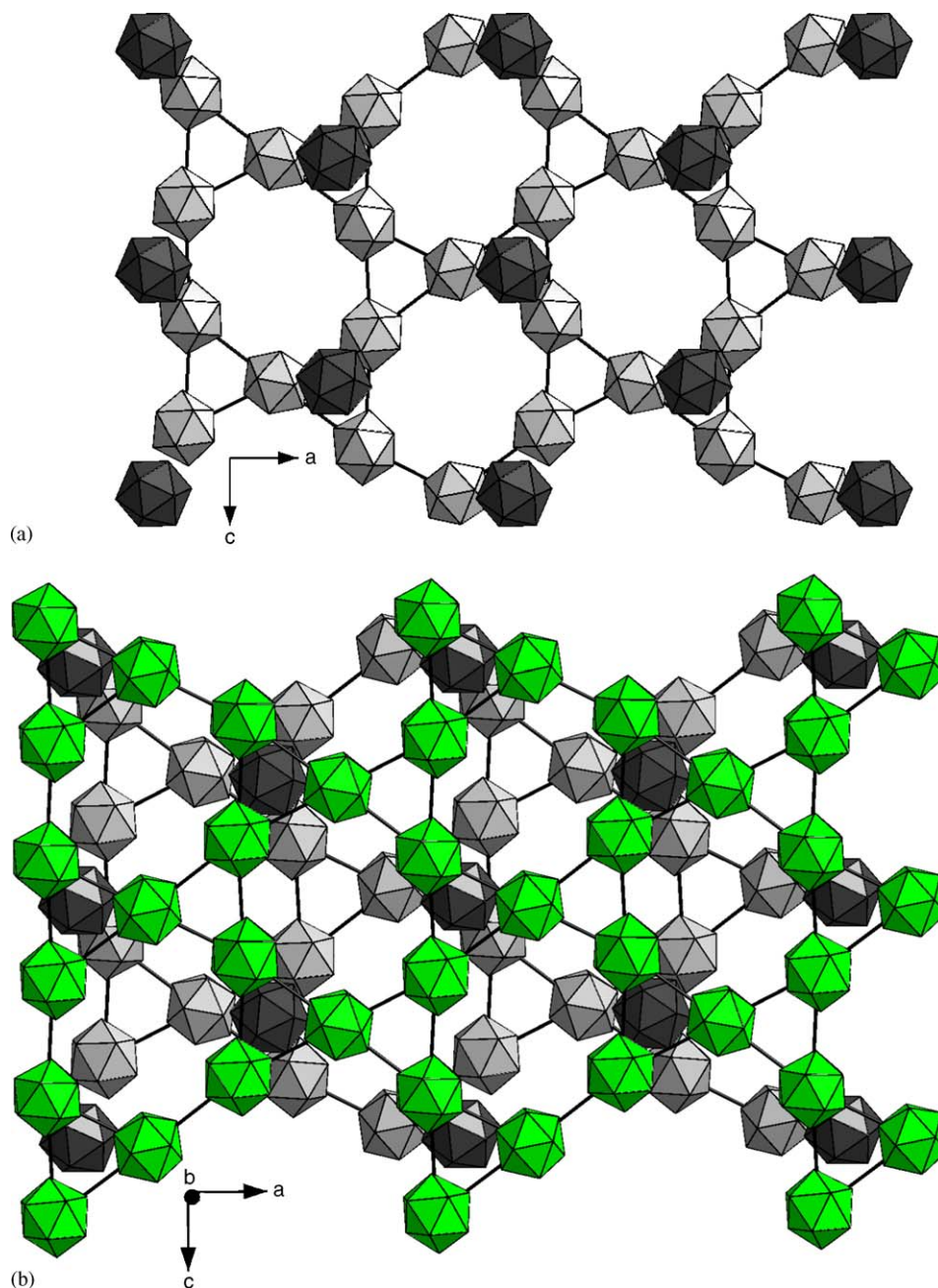


Fig. 4. (a) 3.6.3.6-net (Kagomé net) of icosahedra (light grey; icosahedra 1, 2 and 4) with icosahedra (dark grey: icosahedron 3) connecting the layers (b) stacking of 3.6.3.6-nets.

$B_{21}$  unit has 17 exohedral bonds, 12 to icosahedra and 5 to  $B_{21}$  units. With respect to the centres of the icosahedra the coordination of the  $B_{21}$  unit is a truncated tetrahedron (Friauf-polyhedron).

Alternatively the structure of  $MgB_{12}$  can be seen as a layer structure. The icosahedra 1, 2 and 4 form a 3.6.3.6 net (Kagomé net) in the  $a$ - $c$  plane (Fig. 4a). This motif is frequently found in boron rich borides ( $\alpha$ - $AlB_{12}$  [10],  $\gamma$ - $AlB_{12}$  [11],  $B_{12}Mg_{1.1}Si_2$  [12],  $B_{36}RE_{1-x}Si_{10-y}$  [13],  $B_{36}RE_{1-x}Si_8C_2$  [14],  $B_{36}Mg_3Si_9C$  [12]) and  $\beta$ -rhombohedral boron [15]. One half of the triangles is capped on both sides by the icosahedra 3, connecting the layers in (010)

direction. Neighbouring layers are orientated in a way that above and below the hexagons there are those triangles which are not capped by the icosahedra (Fig. 4b). The voids between the layers formed by one hexagon and one triangle are centered by the  $B_{21}$  units (Fig. 5).

The coordinations for the boron atoms of the icosahedra are quite regular having five endohedral and one exohedral bond to a neighbouring icosahedron or a  $B_{21}$  polyhedron. The values for endohedral bonds vary between 1.700(3) and 1.924(2) Å in agreement with other boron rich borides. The averaged values for the endohedral B-B bonds show small differences between each of the icosahedra (see

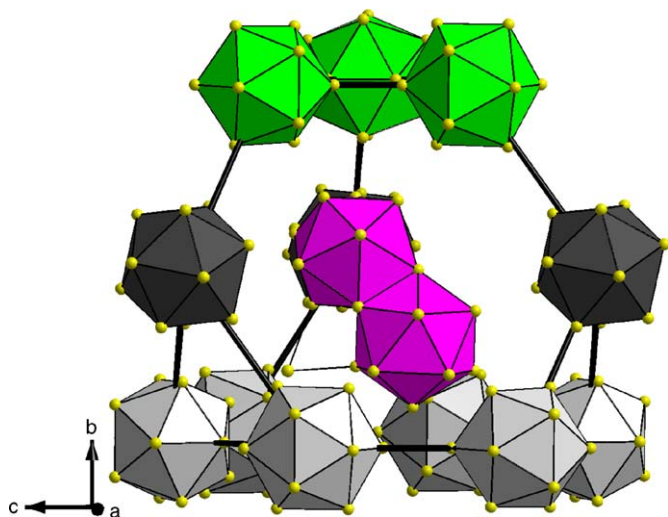


Fig. 5.  $B_{21}$  unit in a void between the layers of icosahedra.

Table 3). The exohedral bonds to  $B_{21}$  units have similar values (1.665(2)–1.934(3) Å) while the exohedral bonds to other icosahedra show more variation (1.599(3)–2.032(2) Å). The deviations for the  $B_{21}$  unit are more pronounced but result from the special geometry. No exohedral but two (B52, B57) or three (B55) additional endohedral bonds are found for the connecting atoms. Two additional endohedral bonds instead of an exohedral bond are also found for B51 and B513 because they are connected to the capping atom B521. All the other boron atoms of the  $B_{21}$  unit have an exohedral bond with a bond length between 1.665(2) and 1.934(2) Å, but one endohedral bond is missing for B16, B18 and B19 because of the missing apex of the icosahedron. The endohedral distances are comparable or slightly longer (1.720(2)–2.050(2) Å) than those found in the icosahedra.

These features are nearly the same as found for the  $B_{20}$  units in  $\alpha$ -AlB<sub>12</sub> [10] and  $\gamma$ -AlB<sub>12</sub> [11] (see below). Usually the exohedral bonds are described as “normal”  $2e2c$  bonds and the endohedral bonds as  $2e3c$  bonds. Therefore, a separation between exohedral and endohedral B–B bonds can be expected as it is found for simple and highly symmetrical borides, for example CaB<sub>6</sub> 1.678/1.751 Å [16] or MgB<sub>7</sub> 1.781/1.841 Å [6]. For MgB<sub>12</sub> a clear separation is not possible probably because of the complexity of the crystal structure. Nevertheless a certain tendency can be observed for the averaged B–B-distances.

As known for most of the boron rich borides the metal atoms show partial occupation and are located in interstices between the boron polyhedra leading to quite irregular coordination spheres. The coordination numbers are between 12 and 16 with Mg–B distances from 2.07 to 2.84 Å in good agreement with other Mg containing boron rich borides [6,8]. Impossible short Mg–Mg distances below 1.0 Å result from partial occupation concerning Mg5 and Mg9.

### 3.2. Comparison to $\alpha$ -AlB<sub>12</sub>, $\gamma$ -AlB<sub>12</sub> and $\beta$ -rhombohedral boron

The crystal structure of MgB<sub>12</sub> is very similar to  $\gamma$ -AlB<sub>12</sub> which shows also a Kagomé net of B<sub>12</sub> icosahedra linked by further icosahedra to a 3D net with additional boron polyhedra in the voids. The main difference is that in AlB<sub>12</sub> there are two different B<sub>20</sub> units instead of the B<sub>21</sub> polyhedra. These B<sub>20</sub> polyhedra can be derived from the B<sub>21</sub> units by removing a second boron atom from the already incomplete icosahedron. Furthermore in  $\gamma$ -AlB<sub>12</sub> the Kagomé nets are slightly corrugated while they are planar in MgB<sub>12</sub>. Although the cell dimensions are nearly the same ( $a = 16.573$  Å,  $b = 17.510$  Å,  $c = 10.144$  Å) the symmetry of  $\gamma$ -AlB<sub>12</sub> is reduced to  $P2_12_12_1$ . According to the  $mnpq$  rules (see below) and the findings of Higashi the B<sub>20</sub> units in AlB<sub>12</sub> need more electrons to get stabilized. Higashi calculated an electron need of 6. By summation of the occupation factors Higashi gave the composition AlB<sub>14.1</sub> for  $\gamma$ -AlB<sub>12</sub> or with respect to the unit cell content Al<sub>25.2</sub>B<sub>352</sub> (Al<sub>6.3</sub>(B<sub>12</sub>)<sub>4</sub>(B<sub>20</sub>)<sub>2</sub>). Similar calculations were done for  $\alpha$ -AlB<sub>12</sub>. In this crystal structure there are B<sub>12</sub> icosahedra and B<sub>20</sub> units in a ratio 2:1, similar to  $\gamma$ -AlB<sub>12</sub>. But in difference to  $\gamma$ -AlB<sub>12</sub> there is only one kind of B<sub>20</sub> polyhedra and the connection of the boron polyhedra is slightly different [17]. The composition from the sum of the Al occupation factors is Al<sub>6.48</sub>B<sub>88</sub> or AlB<sub>13.6</sub>. Compared to magnesium in MgB<sub>12</sub> more electrons are donated by aluminium and the amount of cations is nearly the same. Because of the smaller size of aluminium lattice constants and unit cell volume are reduced in  $\gamma$ -AlB<sub>12</sub>. Therefore our results for MgB<sub>12</sub> are in excellent agreement with Higashi’s investigations on  $\gamma$ -AlB<sub>12</sub> and confirm the validity of the concepts of Jemmis et al. [18] for the stability and electron counting rules for complex boron polyhedra and of Longuet-Higgins and Roberts [19] for the stability of boron polyhedra in solid compounds.

The description of MgB<sub>12</sub> with 3.6.3.6.-Kagomé nets shows a close relationship to the structure of  $\beta$ -rhombohedral boron. In MgB<sub>12</sub> the Kagomé nets of icosahedra are stacked according to a pattern ABAB. The fourth icosahedron connects the triangles to linear chains (Fig. 2) and the B<sub>21</sub> units are above and below the hexagons. In  $\beta$ -rhombohedral boron there are B<sub>12</sub> icosahedra and B<sub>28</sub> units (consisting of three condensed icosahedra) in a ratio 2:1. Three quarters of the icosahedra form a 3.6.3.6-net and the rest of the icosahedra connects the triangles. The sequence of the 3.6.3.6-nets follows a pattern ABCABC (Fig. 6a) so the connection of the icosahedra is three dimensional. The voids above and below the hexagons are occupied by B<sub>28</sub> units (Fig. 6b).

A second description of the crystal structure of  $\beta$ -rhombohedral boron bases on B<sub>84</sub> units built up by a central icosahedron coordinated by 12 half-icosahedra: (B<sub>12</sub>)(B<sub>6</sub>)<sub>12</sub> [20]. The B<sub>84</sub> units are packed in a nearly perfect cubic closest packing. Every B<sub>28</sub> units (see above) gives

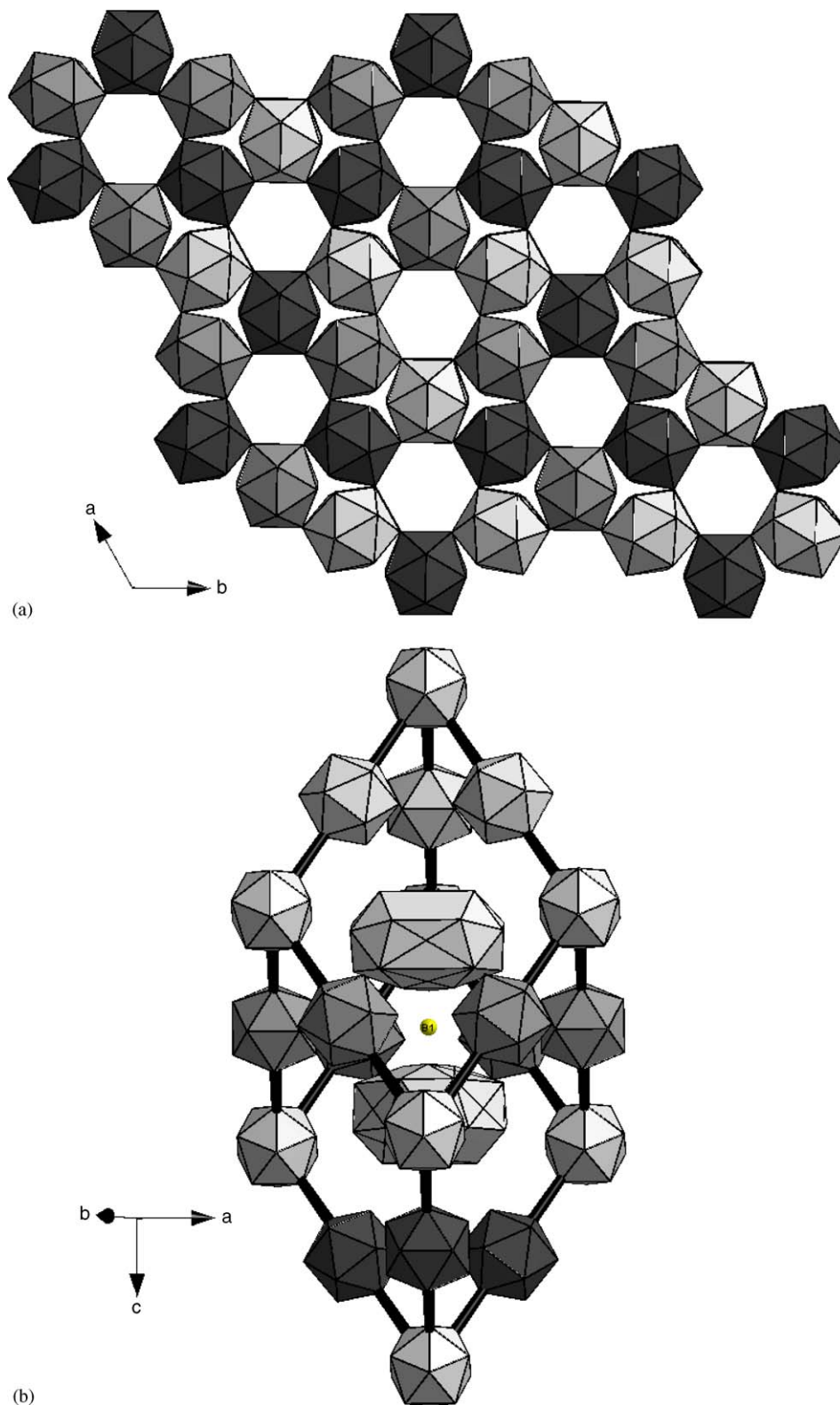


Fig. 6. (a) 3.6.3.6-net of icosahedra in  $\beta$ -rhombohedral boron, sequence ABCABC and (b) connection of the 3.6.3.6-nets by icosahedra and  $B_{28}$  units in voids above and below the hexagons.

three half-icosahedra to the  $B_{84}$  unit, so a  $B_{10}$  fragment remains in a trigonal prismatic void.

In the crystal structure of  $MgB_{12}$  there are  $B_{82}$  units (Fig. 7) which correspond to the  $B_{84}$  units in  $\beta$ -rhombohe-

dral boron with the only difference that two of the half-icosahedra are incomplete:  $(B_{12})(B_6)_{10}(B_5)_2$ . This results from the fact that the six half-icosahedra which coordinate the central  $B_{12}$  icosahedron in the  $a$ - $c$  plane come from the



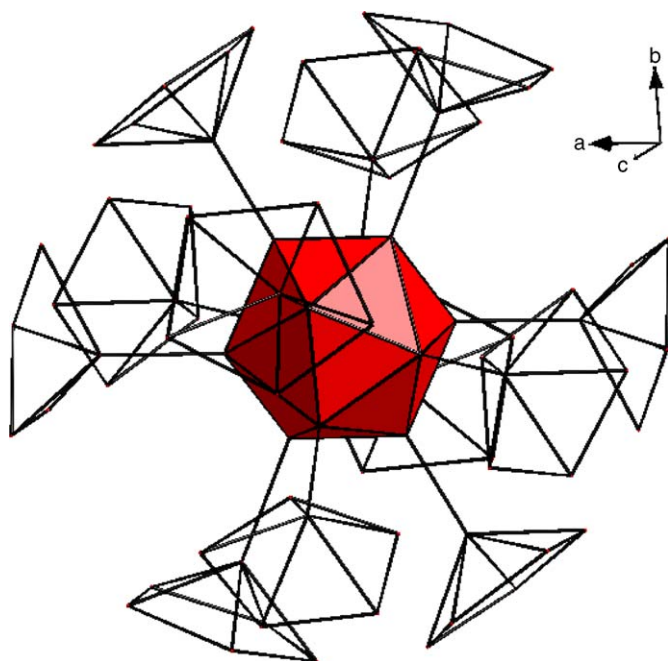


Fig. 7.  $B_{82}$  unit built up by a central  $B_{12}$  icosahedron surrounded by 10 complete half-icosahedra  $B_6$  and two incomplete half-icosahedra  $B_5$  (right and left outside):  $(B_{12})(B_6)_{10}(B_5)_2$ .

$B_{21}$  units. Four of them are from the complete icosahedron while two are from the icosahedron with the missing apex (Fig. 1). The six other half-icosahedra are from the icosahedra 1, 2 and 4, the central icosahedron is icosahedron 3 (see above, Fig. 2). In contrast to  $\beta$ -rhombohedral boron the  $B_{82}$  units form a hexagonal primitive packing with the  $B_{21}$  units in the trigonal voids. Fig. 8 shows that each central icosahedron gets six half-icosahedra from six different  $B_{21}$  units while each  $B_{21}$  unit gives three half-icosahedra to three different  $B_{82}$  units.

### 3.3. Electronic situation in $MgB_{12}$

For a long time bonding in boron polyhedra was in discussion [21]. Since the fundamental work of Wade [22] on the stability of boron polyhedra leading to the Wade rules it is well known that  $B_{12}$  icosahedra as closo-cluster need 2 additional electrons:  $B_{12}^{2-}$ . For nido- and arachno-clusters 4 or 6, respectively, additional electrons are required. This is valid for cases in which each cluster atom performs one exohedral  $2e2c$  bond, i.e. B–H bonds in boranes. For the  $B_{21}$  unit the situation is more difficult. On the basis of the Wade rules, Jemmis et al. [18] developed a model for more complex polyhedra, especially for incomplete, condensed or capped by single boron atoms. According to this model the number of bonding MOs in a closo-, arachno- or nido-cluster is given by an expression  $m+n+o+p-q$  with  $m$  for the number of condensed polyhedra,  $n$  for the number of skeletal atoms,  $o$  for the number of single boron atoms bonded to the cluster,  $p$  for the number of atoms missing with respect to a closo-cluster

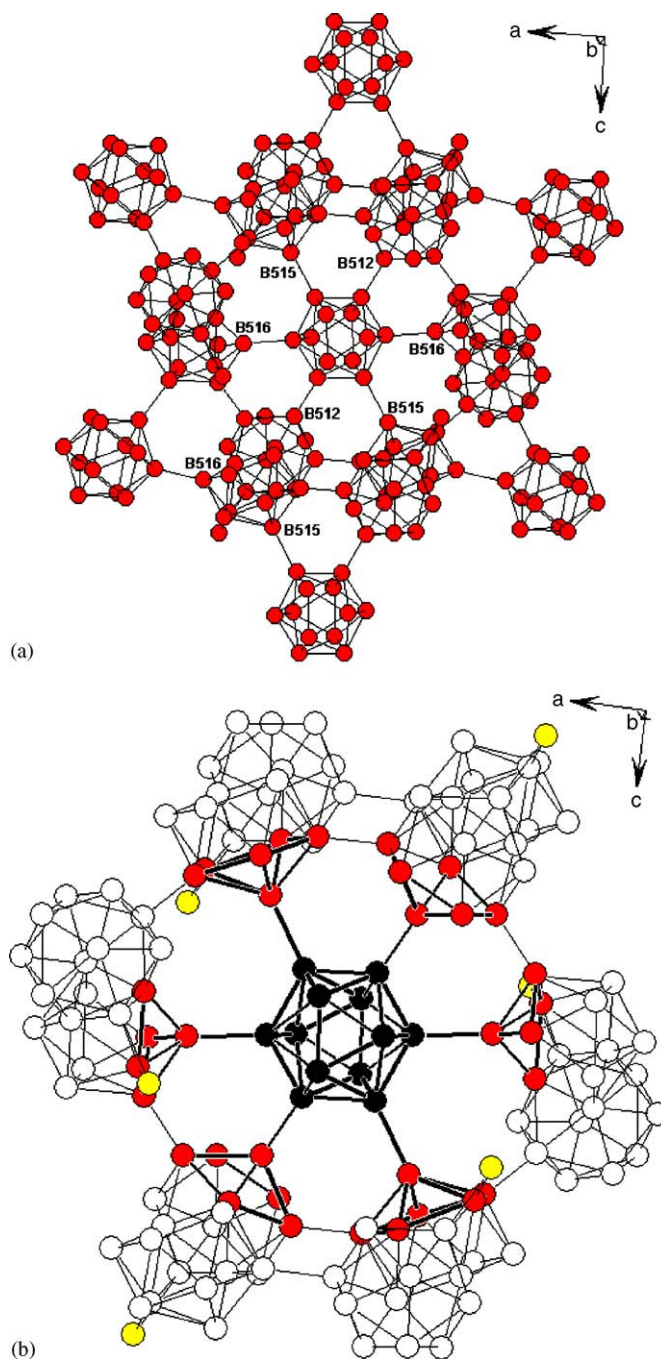


Fig. 8. Connection of the central  $B_{12}$  icosahedron of the  $B_{82}$  unit to the  $B_{21}$  unit (see text).

and  $q$  for the number of boron atoms capping a B–B–B triangle of the cluster. Finally Longuet-Higgins and Roberts [19] have shown that Wade rules can be applied for boron polyhedra in solid state structures. The stability of boron rich borides is mainly determined by an electron transfer of electropositive metal atoms to the framework of the boron polyhedra. The expected amount of electrons to be transferred to stabilize a boron polyhedron depends on its geometry.

An analysis of the boron–boron bonds shows that nearly every boron atom forms one exohedral  $2e2c$  bond. The

only significant exception is B521. Therefore it can be assumed, the Wade rules, its extension by Jemmis and the transfer to solid state compounds by Longuet-Higgins and Roberts are also usable for  $\text{MgB}_{12}$ .

This *mnpq* rule applied to the  $\text{B}_{21}$  unit ( $m = 2, n = 21, o = 1, p = 1, q = 0$ ) gives 25 electron pairs. Regarding the 17 exohedral  $2e2c$  bonds the  $\text{B}_{21}$  unit requires 67 electrons. Because  $3 \times 21 = 63$  electrons are from the boron atoms, 4 additional electrons are needed and should be supplied by the Mg atoms. The unit cell of  $\text{MgB}_{12}$  contains 16  $\text{B}_{12}$  icosahedra and 8  $\text{B}_{21}$  units. Therefore, the framework of the boron polyhedra needs 64 electrons. The crystal structure contains about 29.15 Mg atoms which is in excellent agreement with the expected value regarding the simplicity of the model and the complexity of the crystal structure.

The application of the *mnpq* rule to  $\alpha\text{-AlB}_{12}$  and  $\gamma\text{-AlB}_{12}$  leads to an electron need of 6 for the  $\text{B}_{20}$  unit ( $m = 2, n = 20, o = 1, p = 2, q = 0$ ) as it was already stated by Higashi [10,17]. The observed Al contents are in good agreement. For the unit cell of  $\gamma\text{-AlB}_{12}$  with 16 icosahedra and 8  $\text{B}_{20}$  units 80 electrons are required. The observed content are 25.2 Al atoms (75.6 electrons). For  $\alpha\text{-AlB}_{12}$  with a real composition  $\text{AlB}_{13.6}$  and half the unit cell volume 12.8 Al atoms (38.4 electrons) are found.

If the boron polyhedra framework of  $\gamma\text{-AlB}_{12}$  should be stabilized by magnesium about 38 Mg atoms would be required and the expected composition is  $\text{MgB}_{9.3}$ . A careful analysis of the Al positions in  $\gamma\text{-AlB}_{12}$  shows that only 36 atoms can be placed into the crystals structure without forcing unusual short Mg–Mg contacts. This might be the reason for the formation of the  $\text{B}_{21}$  units in  $\text{MgB}_{12}$ . According to the *mnpq* rules the  $\text{B}_{21}$  unit demands fewer electrons than the  $\text{B}_{20}$  unit. Therefore, the electrons, which are necessary for the stabilization can be supplied by a metal with fewer valence electrons.

The important role of electronic factors can be shown by several other examples. Higashi et al. [23] reported on a ternary compound  $\text{Al}_{1.4}\text{Mg}_{0.45}\text{B}_{22}$  (chemical analysis) or  $\text{Al}_{1.2}\text{Mg}_{0.47}\text{B}_{22}$  (X-ray data) respectively, with the structure of  $\gamma\text{-AlB}_{12}$ . Here the number of electrons per unit cell coming from the metal atoms can be calculated to 72.6 up to 81.6. Recently [24] we yielded single crystals of “ $\text{AlB}_{17}$ ” with an identical boron framework as it was found in  $\text{MgB}_{12}$ . Here the unit cell contains 21.13 Al atoms corresponding to a number of 63.4 electrons. Furthermore we were able to substitute a part of the Mg atoms in  $\text{MgB}_{12}$  by lithium [25].

According to preliminary results the single crystalline samples are non-superconducting down to 2 K [26].

#### 4. Summary

The existence of a binary compound  $\text{MgB}_{12}$  was claimed in an early work in 1955 by Markovski et al. [4]. It was stated in a recent work that a compound with a composition  $\text{MgB}_{12}$  could not be synthesized from the

elements [5]. By use of a Cu/Mg melt we were able to obtain single crystals of  $\text{MgB}_{12}$ . Structure solution and refinement were done with single crystal data resulting in the composition  $\text{MgB}_{12}$  which was confirmed by WDX measurements. The crystal structure is similar to  $\gamma\text{-AlB}_{12}$  and consists of  $\text{B}_{12}$  icosahedra and  $\text{B}_{21}$  units in a ratio 2:1. These  $\text{B}_{21}$  units which are here observed for the first time are built of two condensed icosahedra with one missing apex and an additional boron atom. The content of 7.3 magnesium atoms we have found in the formula unit corresponds nearly to the expected value of 8 which can be explained by the required number of electrons to stabilize the boron polyhedra  $[(\text{B}_{12})^{2-}]_4$  and  $[(\text{B}_{21})^{4-}]_2$ .  $\text{MgB}_{12}$  is a convincing example for the stabilization of 3D networks of boron polyhedra by the uptake of electrons from suitable metal atoms. The electron need can be derived directly from the geometry of the corresponding polyhedra. Especially the comparison to  $\gamma\text{-AlB}_{12}$  with its similar but not identical crystal structure supports the *mnpq*-concept developed by Jemmis et al. [18] for complex boron polyhedra.

#### Acknowledgments

Thanks are due to the Bayerisches Geo-Institut (BGI, Universität Bayreuth) for the access to WDX measurements and to Detlev Krauß for his support.

This work was supported by the program “Neue Werkstoffe in Bayern”, project B21092.

#### References

- [1] J. Nagamatsu, N. Nakagawa, T. Muranaka, Y. Zenitani, J. Akimitsu, *Nature* 40 (2001) 63–64.
- [2] (a) S. Gunji, H. Kanimura, *Phys. Rev. B* 54 (1996) 13665–13673;  
(b) K. Soga, A. Oguri, S. Araake, K. Kimura, M. Terauchi, A. Fujiwara, *J. Solid State Chem.* 177 (2004) 498–506.
- [3] H. Okamoto, *Phase Diagrams for Binary Alloys*, ASM, Ohio, 2000.
- [4] L.Y. Markovski, Y.D. Kondrashev, G.V. Kapuatsvskaya, *J. Gen. Chem. USSR* 25 (1955) 409–416.
- [5] S. Brutti, M. Colapietro, G. Calducci, L. Barba, P. Manfrinetti, A. Palenzona, *Intermetallics* 10 (2002) 811.
- [6] V. Adasch, K.-U. Hess, Th. Ludwig, N. Vojteer, H. Hillebrecht, *J. Solid State Chem.*, in press, doi:10.1016/j.jssc.2006.03.009.
- [7] A. Guette, M. Barret, R. Naslain, P. Hagenmuller, L.-E. Tergenius, T. Lundström, *J. Less-Common Metals* 82 (1981) 325–334.
- [8] V. Adasch, Ph.D. Thesis, University of Bayreuth, Germany, 2005.
- [9] G.M. Sheldrick, *Programme SHELXL*, University of Göttingen, Germany, 1997.
- [10] I. Higashi, T. Sakurai, T. Atoda, *J. Solid State Chem.* 20 (1977) 67–77.
- [11] (a) I. Higashi, *J. Solid State Chem.* 47 (1983) 333–349;  
(b) R.E. Hughes, M.E. Leonowitz, J.T. Lemley, L.-T. Tai, *J. Am. Chem. Soc.* 99 (1977) 5507.
- [12] T. Ludwig, H. Hillebrecht, contribution to 15th International Symposium on Boron, Borides and Related Materials, ISBB05, 21.–26.8.2005, Hamburg, Germany.
- [13] F.X. Zhang, F.F. Xu, T. Mori, Q.L. Liu, T. Tanaka, *J. Solid State Chem.* 170 (2003) 75–81.

- [14] J.R. Salvador, D. Bilc, S.D. Mahanti, M.G. Kanatzidis, *Angew. Chem.* 114 (2002) 872–874 (*Angew. Chem. Int. Ed. Engl.* 41 (2002) 844–846).
- [15] G.A. Slack, C.I. Hejma, M.F. Garbaskas, J.S. Kasper, *J. Solid State Chem.* 76 (1988) 52–63.
- [16] F. Meyer, Diploma Thesis, University of Freiburg, Germany, 1997.
- [17] I. Higashi, *J. Solid State Chem.* 154 (2000) 168–176.
- [18] E.D. Jemmis, M.M. Balakrishnarajan, P.D. Pancharatna, *J. Am. Chem. Soc.* 123 (2001) 4313–4323.
- [19] H.C. Longuet-Higgins, M.V. Roberts, *Proc. Roy. Soc. Lond. Ser. A* 230 (1955) 110.
- [20] V.I. Matkovich, R.F. Giese, *J. Economy, Z. Kristallogr.* 122 (1965) 116–130.
- [21] W.N. Lipscomb, *Adv. Inorg. Chem. Radiochem.* 1 (1950) 117.
- [22] K. Wade, *Adv. Inorg. Chem. Radiochem.* 18 (1976) 1.
- [23] I. Higashi, M. Kobayashi, Y. Takahashi, S. Okuda, K. Hamano, *J. Crystal Growth* 99 (1990) 998–1004.
- [24] N. Vojteer, Th. Ludwig, H. Hillebrecht, unpublished results.
- [25] N. Vojteer, Diploma Thesis, University of Freiburg, Germany, 2005.
- [26] H. Hillebrecht, K. Erb, unpublished results.